CERN-INTC-2024-017 / INTC-P-696
10/01/2024

EUROPEAN ORGANIZATION FOR NUCLEAR RESEARCH

Proposal to the ISOLDE and Neutron Time-of-Flight Committee

Magnetic origins of epitaxial MAX phase Mn_2GaC-based thin films probed by Emission Mössbauer Spectroscopy

[submission date: 10.01.2024]

B. Qi[1], H. P. Gunnlaugsson[1], S. Olafsson[1], E. B. Thorsteinsson[1], F. Magnus[1], J. Rosen[2], Q. Tao[2], R. Mantovan[3], H. Masenda[4], D. Zyabkin[5], J. Schell[6], K. Bharuth-Ram[7], The Mössbauer collaboration at ISOLDE/CERN[8]

[1]Science Institute, University of Iceland, Iceland; [2]Materials Design, Department of Physics, Chemistry and Biology (IFM), Linköping University, Sweden
[3]CNR-IMM, Unit of Agrate Brianza, Via C. Olivetti 2, 20864 Agrate Brianza (MB), Italy
[4]School of Physics, University of the Witwatersrand, South Africa
[5]TU Ilmenau, Ilmenau, Germany; [6]ISOLDE, CERN, Geneve, Switzerland
[7]School of Physics,University of KwaZulu-Natal, Durban, South Africa
[8]https://ems.web.cern.ch/content/collaborators

Spokesperson(s): B.Qi (bingcui@hi.is) and Q. Tao (quanzheng.tao@liu.se)
Local contact: J. Schell (juliana.schell@cern.ch)

Abstract

MAX phase is a class of nanolaminated materials composed of a transition-metal (M), an A-group element (A) and C or N (X). The possibility to tune the magnetic properties of MAX phase thin films through atomic substitution, introduction of strain, temperature, or external magnetic field is important to optimize different functionalities of these materials. We propose a detailed study of Mn_2GaC-based MAX phase thin films with emission Mössbauer spectroscopy (eMS) to elucidate the detailed nature of the magnetic structure and the non-trivial magnetic interactions in these films. Through eMS as performed at $^{57}Fe/^{119}Sn$ sites by following implantation of radioactive parents ^{57}Mn and ^{119}In at various temperature, and at the adopted ultra-diluted regime, the micro-structure and magnetism of the thin films can be probed at the atomic scale, thus providing opportunities to explore the magnetic properties of these systems at substitutional atomic lattice sites. As a result, a direct correlation of the local chemical order in the M- and/or A-layers and the disorder on the M- and A-sites with the rich magnetic phase diagram of the Mn_2GaC-based MAX phase films can be established.

Requested shifts: 7 shifts (split into 2-3 runs over ~2 years)

1 INTRODUCTION

MAX phase is a family of inherently nanolaminated materials, composed of a transition metal (M), an A-group element (A) and either carbon or nitrogen (X) with the chemical formula $M_{n+1}AX_n$ (n = 1–3). Owing to the laminated structure, and the alternating strong covalent M-X bonds, and the weaker ionic and metallic M-A bonds, the materials combine the features of metals and ceramics, showing promise as a wide range of structural and functional materials [1]. The feasibility of attaining MXenes, an emerging family of graphene-like 2D materials, via MAX phase, has also enhanced the research on the MAX phase [2,3]. Guided by the theoretical modelling and phase stability predictions, at least 342 MAX phases have been synthesised to date, and more awaiting to be discovered [4]. Furthermore, the interest in low-dimensional magnetism has fuelled the search for new MAX phases exhibiting magnetic order with magnetic elements in the form of Mn, Cr, or Fe on the M-site or Mn, Fe, Co, and/or Ni on the A-site for spintronic applications [5-8].

The most studied of the magnetic MAX phases is Mn_2GaC because of its rich tuneable magnetic diagrams. It exhibits non-collinear (ferromagnetic-like (FM-like)) magnetic ordering with a sizable remanent magnetization below 210 K, where it undergoes a magnetic phase transition to an antiferromagnetic (AFM) ordering at higher temperatures [5]. The magnetic phase transition coincides with a first-order structural phase transition, where an abrupt change in the c-axis lattice parameter by 0.2 % with an asymmetric change of the crystal structure takes place. The coupled magnetic and structural phase transition can also be induced by applying a magnetic field above 210 K. The magneto-structural transformations in the Mn_2GaC film as a response of temperature and external magnetic field applied parallel to the film plane is summarized in Fig.1 [7].

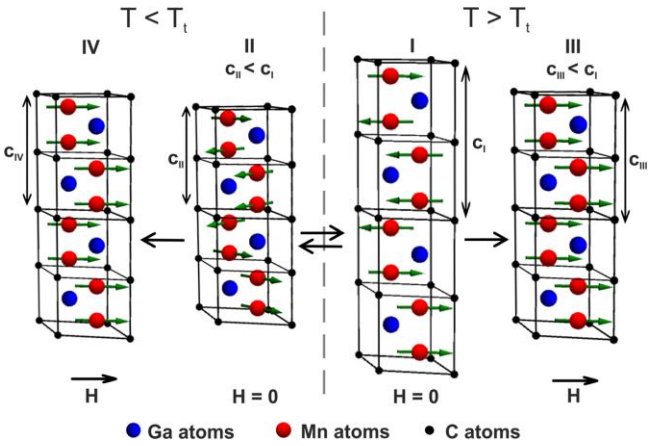

Fig.1. Schematic representation of magneto-structural transformations in the Mn_2GaC film as a response of temperature and external magnetic field applied parallel to the film plane. (I) At $T > T_t$ = 214 K the system has an AFM $[0001]_4^A$ magnetic spin configuration and respective spin alignment between magnetic sublattices is collinear. (II) At $T < T_t$ = 214 K the Mn_2GaC undergoes the first order phase transition, which is characterized by *c*-axis lattice compression ($C_{II} < C_I$) and magnetic spin transformation to a non-collinear AFM $[0001]_4^A$ state, which gives the metamagnetic properties of the material. (III) at $T > T_t$ an external magnetic field causes the parallel spin alignment and compression of the lattice along the *c*-axis ($C_{III} < C_I$) delivering large negative magnetostriction of −450 ppm. (IV) At $T < T_t$ parallel spin configuration causes large positive magnetostriction of 450 ppm ($C_{IV} > C_{II}$) [7].

This complex magnetic behaviour as the function of temperature and applied magnetic field is a result of competing magnetic interactions within the M–X–M trilayers and across the A layers as indicated by first-principles calculations and Monte Carlo simulations [10,11]. However, the magnetic structure below the transition point is still an on-going research subject. The zero-field ^{55}Mn Nuclear Magnetic Resonance

(NMR) study indicates the presence of magnetically non-equivalent Mn sites within this structure [12]. The average magnetic moment of Mn was found around 2 μB, strongly contrasting with the reported remanent magnetization of only 0.3 μB measured with vibrating sample magnetometer (VSM) at zero-field below 50 K [10]. The nuclei of non-magnetic Ga atoms were shown to experience the transferred hyperfine magnetic field of 15.75 T (±0.05 T), evidencing the presence of an uncompensated FM moment within the Mn sublattice, and suggest their non-collinear arrangement across the Ga layer [12]. With the same NMR measurements performed in an external magnetic field up to 1 T, a helical spiral magnetic structure consisting of the ferromagnetically coupled Mn-C-Mn slabs that are twisted across the Ga layer by 167.2° with respect to the next Mn-C-Mn slab was demonstrated. Thus, the magnetic structure of MAX phase MnGaC was globally represented as a spiral propagating along the out-of-plane direction (hexagonal *c* axis) with a pitch of around 14 lattice constants [13]. These findings are fully consistent with the Monte Carlo calculation results, which predict FM exchange interaction (J_1) between the first nearest neighbors, and AFM exchange interaction (J_2) between every second supermoment layer [10,11]. The different magnetic moment value of Mn obtained with NMR and VSM indicates that the spins of Mn atoms could be locally aligned but macroscopical oriented in the different domains.

Theoretic study on the effect of substitution of Mn and Ga atoms by Fe atom on the magnetic properties of the Mn_2GaC MAX phase found that only FM ordering is possible when Fe atom ordering over Ga sites. It is the out-of-plane Fe-Mn exchange that gives the main contribution in appearance of FM phase. The temperature dependences of magnetization reveal the increase of Curie temperature in Mn_2GaC with Fe atom incorporated into Ga-site [14]. We have synthesized the $(Mn,Fe)_2GaC$ MAX phase, which didn't show FM properties with VSM measurement.

These results strongly indicate that the magnetic properties of the MAX phase material are closely associated with the in-plane local site of the M and A elements as well as the out-of-plane M-A exchange interactions in the laminated structures. Therefore, it is important to understand the effects of both the lattice site and the interlayer interaction of M and A elements on the magnetic properties of the MAX phase material to fine tun the magnetic properties by chemical composition, order, and crystal structure. These point a high necessity of applying the local probes like emission Mössbauer spectroscopy (eMS).

2 EXPERIMENTAL PLAN

2.1 Samples and pre-characterization

The crystal structure of Mn_2GaC can be described as hexagonal unit cells of the Mn_6C octahedral of the P63/mmc space group, interleaved with single 2D layers of Ga element. Fig.2 shows the pole figure at $2\theta=41.84^\circ$ for the $(10\bar{1}3)$ peak of the single orientated (0006) Mn_2GaC and 51% $(10\bar{1}3)$ and 49% (0006) oriented $Mn_{0.88}C_{0.12}GaC$ MAX phase thin films grown by direct current magnetron

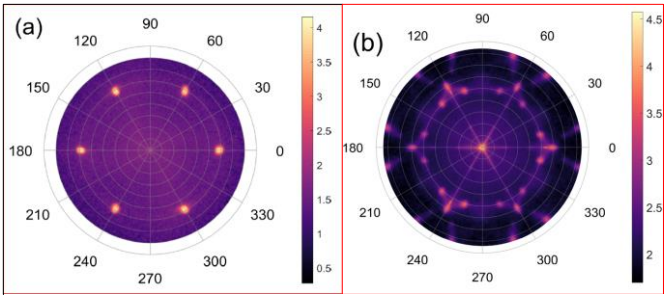

Fig.2. Pole figure at $2\theta = 41.84^\circ$ for the $(10\bar{1}3)$ peak of (a) single orientated (0006) Mn_2GaC film [4] and (b) 51 % $(10\bar{1}3)$ and 49 % (0006) oriented $Mn_{0.88}C_{0.12}GaC$ film [9].

sputtering (dcMS) on 1×1 cm^2 MgO (111) substrates. The single-crystal nature of the film can be seen from the discrete sixfold symmetric points.

Fig.3 highlights the metamagnetic transition of the in-plane magnetic response of the Mn_2GaC film above the phase-transition temperatures induced by the magnetic field. The inset shows out-of-plane magnetization measurements at the same temperatures. At low temperatures the film exhibits FM-like behaviour with a significant remanent magnetization of 0.18 μB/Mn atom. At ~210 K a magnetic phase transition occurs to an AFM state, but a metamagnetic transition is observed at increasingly high fields with increasing temperature [8].

Fig.4 highlights the strong magnetization of $(Mn_{1-x}Cr_x)_2GaC$ series. With x = 0.12, the highest saturation magnetization of 1.25 μB/M-atom at 3 K and maintain 0.90 μB/M-atom at 300 K was obtained. This is the first MAX phase, which shows strong FM at room temperature, with great scope for further tuning of its magnetic properties through compositional doping.

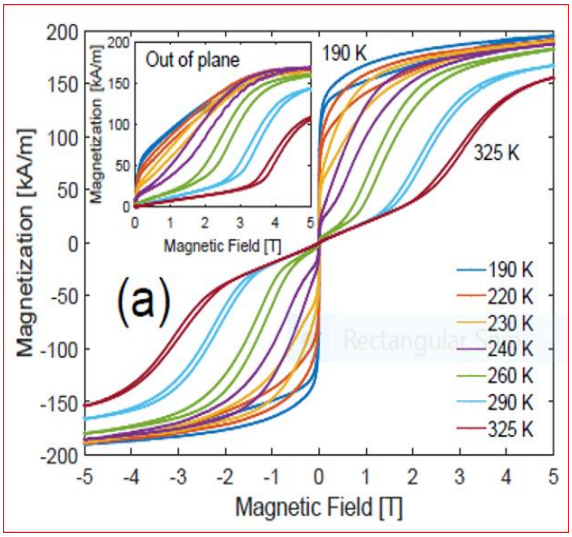

Fig.3. In-plane magnetization measurements for selected temperatures above and below the magnetic phase transition of the single orientated (0006) Mn_2GaC film, the inset showing out-of-plane measurements. All the measurements have had the MgO background subtracted [8].

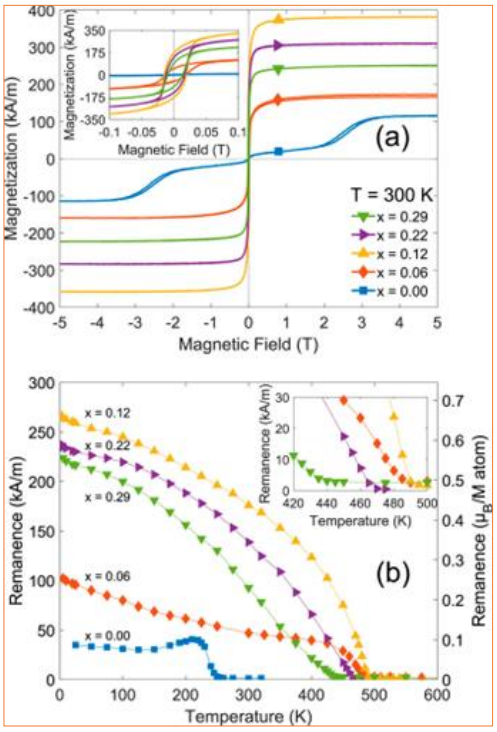

Fig.4. (a) Magnetic hysteresis loops for all the $(Mn_{1-x}Cr_x)_2GaC$ samples at 300 K. The sample with x = 0.00 refers to Mn_2GaC which has the distinctive metamagnetic transition seen in Fig.3, with increasing Cr content, a typical ferromagnetic response is obtained. The inset shows a zoomed-in view of the hysteretic part of the loop, demonstrating a large remanent magnetization for all Cr containing samples. All the measurements had the MgO background subtracted. (b) Remanent magnetization as a function of temperature for the sample series. The inset shows a zoomed-in view of the critical temperature region. Samples with x = 0.12 and above, and the magnetization is largest for x = 0.12 [9].

2.2 Emission Mössbauer spectroscopy (eMS) characterization

The main characterization technique in this proposal is ^{57}Fe and ^{119}Sn eMS following implantation of ^{57}Mn ($T_{1/2}$ = 1.45 min.) and ^{119}In ($T_{1/2}$ = 2.4 min.), respectively. The samples are held in a multi-purpose implantation

chamber [15] and the 14.4 keV and 23.9 keV γ-ray emission is measured with a resonance detector equipped with ^{57}Fe in a stainless steel or $Ca^{119}SnO_3$ electrode mounted on a conventional Mössbauer drive system outside the implantation chamber.

Mössbauer spectroscopy (MS) gives amongst others, the following quantities, relevant for the current proposal [16]

- The position of resonances gives information on the electron charge density at the nucleus ($|\psi(0)|^2$) which can be used to determine the charge/spin state of the Fe (Mn)/Sn (Ga) probe site.
- The relative intensity of the spectrum which is related to the Debye-Waller factor can be used to distinguish the probe entering the regular lattice site or the interstitial or damage sites.
- Quadrupole splitting of spectral components originated from the orbital population and site symmetry of the probe nuclei can be used to determine the crystal structure of the probe site.
- Magnetic interactions characterized by splitting of resonance lines into 6 individual lines in the case of ^{57}Fe and ^{119}Sn can give simultaneously information on the magnetic properties of the material and site symmetry.
- Temperature-dependent site populations can be used to study the nature of intrinsic or post-implantation induced lattice defects in the crystal structure and co-related magnetic properties of the material.

There are two main properties that eMS using ^{57}Mn and ^{119}In isotopes at ISOLDE is superior to conventional MS using doped samples: (1) The concentration required (<10^{-3} at. %) is a fraction of what is required for MS (~0.1 at. %) and (2) the timescale of the experiments is minutes with eMS compared to days with MS. Both these properties eliminate the possibility of precipitation and one can safely assume that the Mn/Fe and In/Sn are dilute in the samples.

This technique has been successfully used to correlate the Mn and Ga site-specific chemical, structural, and magnetic properties of binary Heusler alloy Mn_xGa, as a function of x, with the macroscopic magnetisms measured by superconducting quantum interference device magnetometry. Hyperfine magnetic fields of Mn/Fe (at Mn or Ga sites) are found to be quite sensitive to the local strain induced by the implantation. However, In/Sn probes are much less sensitive to the strain state as well as to the local distortions induced by the implantation damage than the ^{57}Fe probe atoms [17]. With this in mind, we tested the possibility of the ^{57}Mn eMS to study the MAX phase Mn_2GaC thin film during the Mn beam-time in 2023 at ISOLDE. Fig.5 shows the first set of eMS results of the MAX phase Mn_2GaC thin film. The sample was cooled by cooling the sample holder constantly with the liquid N_2 from 300 K to 100 K. The spectra were measured without an applied magnetic field.

From visual inspection of the spectra, we can observe that, there is a broad transition centred at temperature ~210 K. The spectra at 302 K and 246 K both show a broad feature centred at isomer shift δ ~ 0 - 0.3 mm/s indicating dominantly Fe^{3+} paramagnetic state and a broad feature. It could be interpreted as magnetic feature owing to Fe with magnetic moment up to 1 μB, or due to unresolved quadrupole interaction or implantation-induced internal stresses/strains which altered magnetic order as noted in ref. [17]. These possibilities can be distinguished with further angular dependent measurements with and without external magnetic field, and post-implantation annealing measurement.

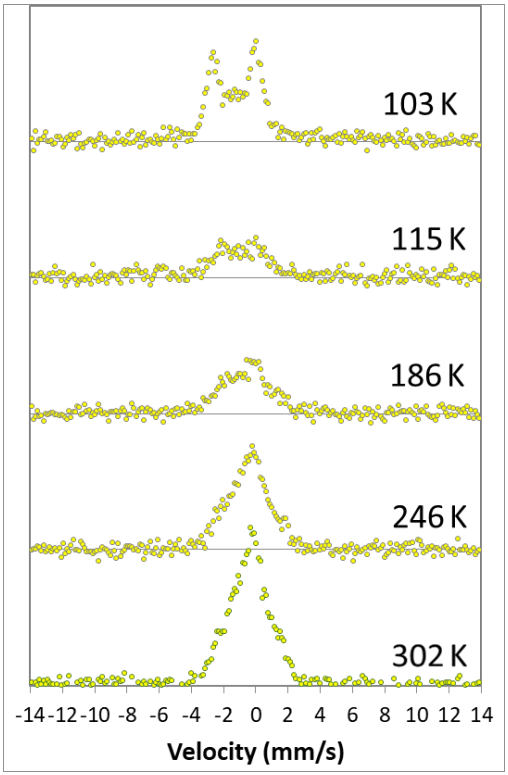

Fig.5: Primary ^{57}Mn eMS spectra of the Mn_2GaC MAX phase thin film measured at the temperature as indicated in a full range of velocity scale.

We can also tentatively compare our observations with the eMS results obtained on the MnxGa samples (x = 0.7-1.9) in ref. [17]. It was found that as a general trend, the contribution of the magnetic hyperfine fields from Fe/Mn probe on Mn site and Ga site in MnxGa alloy to the emission spectra gradually diminished as x increases. With x = 1.9, i.e. for Mn_2Ga, the ^{57}Mn eMS spectra didn't show clear magnetic splitting, which could be due to crystal imperfection and formation of phases with slightly altered preferential orientation, and implantation-induced internal stresses/strains in the compound. However, as the crystal structure, chemical order/bond and electronic band structure of Mn and Ga atoms in MnxGa alloys and MAX phase Mn_2GaC are completely different, to fully understand the eMS results we obtained and to gain a deep understanding about how the nanolaminated structures in the MAX phase Mn_2GaC interrelate with the rich magnetic properties of this material, further study with both ^{57}Mn and ^{119}In eMS are highly desired.

The spectra at 186 K and 115 K show a weakening of the central peak and an enhancement of the apparent sextet feature. The spectral area in Mössbauer spectroscopy depends on the temperature-dependent Debye-Waller factor, which in first approximation decreases exponentially with temperature, a behaviour that is not represented in the experimental data. Secondly, the compression of the lattice below 210 K (state II compared to state I in Fig. 1) would expect an increased spectral area, also opposite to what is measured experimentally. This suggests that the bond strength in the crystal structure of MAX needs deep understanding.

The sudden emergence of a new peak area below 115 K is most probably due to ice forming on the surface of the sample below 115 K due to technical reasons. This should be verified thoroughly with further eMS measurement performed at both the high and low temperatures. As also pointed out by the eMS results obtained on the MnxGa samples in ref. [17], the implantation damage at low temperature can be completely annealed at 295 K and beyond, and before reaching the Curie-T, the magnetic features became more visible over the damage. High temperature measurements are likewise very much needed to study the structure-related magnetic properties of the MAX phase material.

Considering the possibility to tune the magnetic properties through atomic substitution, doping, introduction of strain, temperature, and external magnetic field to optimize different functionalities of these thin films, further study on the local lattice structure and element-correlated magnetic properties is required to elucidate the delicate nature of the magnetic structure and to understand the non-trivial magnetic interactions in these exotic magnetic MAX phase thin films. In this regard, the Mössbauer effect

by the ^{57}Fe/^{119}Sn sites following implantation of radioactive ^{57}Mn and ^{119}In at various temperature can be used to probe the micro-structure and the site-related magnetism of the MAX phases with the Mn_2GaC-based thin films as protocol samples. As a result, a direct correlation between the local structure and the rich magnetic phase diagram (and other physical or electrical properties) of the MAX phase thin films could be established, and externed to identify the new interesting magnetic MAX phases.

Therefore, we propose further eMS study at ISOLDE on the Cr-doped and undoped Mn_2GaC MAX phase thin films at full temperature series, below and above the room temperature (RT). For specific cases, isothermal annealing studies using so-called time delayed measurements [18] is required. We have the permanent magnets that can give external magnetic field of 0.6 T, parallel to the sample surface normal. A low temperature magnet can be constructed based on the cold lid we already have to cool the sample to low temperatures. With eMS data collected in the external magnetic field (with optional cooling), the expected magnetic splitting per Mn/Fe atom in the structure can be verified.

2.3 Post characterization

The temperature induced crystal structure changes in phase transition can be followed by the X-Ray diffraction facilitated with in-situ annealing at our home institute. Theoretical study can be performed by the experts within the collaboration group.

3 CONCLUSIONS/OUTLOOK

Our first attempt to study the MAX phase with eMS in 2023 has proved that the MAX phase is suitable for eMS studies using implantation. Upon completion of this project, we will be able to

- Gain deeper understanding of the local chemical order, composition, and structure-correlated magnetic properties of the materials, which will allow to propose better ways to design the new magnetic MAX phase material through compositional doping.
- Document the changes in the nature of the probe site at low and high temperatures, both with respect to magnetic interaction and the local site structure properties.

To fully understand the system, we need to use ^{57}Mn eMS at low and high temperatures (~4 h per sample), rotation at RT with and without magnetic field parallel and perpendicular to the surface (1.5 h per sample per external field, 6.5 h total per sample) and implantation at low temperatures (~2 h). Complete characterization is therefore expected to be around 9.5 hours per sample. We will apply ^{57}Mn to Mn_2GaC, $(Mn_{0.88}Cr_{0.12})_2GaC$, and one additional composition depending on the results. Then we will apply the ^{119}In to the samples which the ^{57}Mn data suggests importance to get data. Together with calibration (10%) and contingency/further exploration (20%) we will need min. 4.5 Mn and 2.5 In shifts.

Table 1. Summary of requested shifts

Beam	Min. Intensity	Energy	Target/Ion source	Samples	Shifts
^{57}Mn	$1.5\cdot10^8$ ions/s	≥50 keV	UC_2/RILIS	Mn_2GaC+$(Mn_{1-x}Cr_x)_2GaC$(x=0.12…)	4.5
^{119}In	$1.5\cdot10^8$ ions/s	≥50 keV	UC_2/RILIS	Mn_2GaC+$(Mn_{1-x}Cr_x)_2GaC$(x=0.12…)	2.5

References:

1. M.W. Barsoum, T. El-Raghy, The MAX phases: unique new carbide and nitride materials, Am. Sci., 89 (2001)334
2. J. Wozniak, A. Jastrzębska and A. Olszyna, Challenges and opportunities in tailoring MAX phases as a starting materials for MXenes development, Materials Technology, 37:11(2022)1639-1650, https://DOI: 10.1080/10667857.2021.1968102.
3. J. Zhou, M. Dahlqvist, J. Bjork and J. Rosen, Atomic Scale Design of MXenes and Their Parent Materials_From Theoretical and Experimental Perspectives, Chem. Rev. 123(2023), 13291−13322, https://doi.org/10.1021/acs.chemrev.3c00241.
4. M. Dahlqvist, M. W. Barsoum and J. Rosen, MAX phases – Past, present, and future, Materials Today (2023), https://doi.org/10.1016/j.mattod.2023.11.010
5. A.S. Ingason, A. Petruhins, M. Dahlqvist, F. Magnus, A. Mockute, B. Alling,L. Hultman, I.A. Abrikosov, P.O.Å. Persson and J. Rosen, A nanolaminated magnetic phase: Mn_2GaC, Mater. Res. Lett., 2(2013)89, https://DOI:10.1080/21663831.2013.865105.
6. A. S. Ingason, M. Dahlqvist and J Rosen, Magnetic MAX phases from theory and experiments; a review, J. Phys.: Condens. Matter, 28(2016)433003, https:/doi:10.1088/0953-8984/28/43/433003.
7. L. P. Novoselova, A. Petruhins, U. Wiedwald, A. S. Ingason, T. Hase, F. Magnus, V. Kapaklis, J. Palisaitis, M. Spasova, M. Farle, J. Rosen and R. Salikhov, Large uniaxial magnetostriction with sign inversion at the first order phase transition in the nanolaminated Mn_2GaC MAX phase, Sci. Rep., 8 (2018), p. 2637. https://DOI:10.1038/s41598-018-20903-2.
8. E.B.Thorsteinsson,A.S.Ingason and F. Magnus. Magnetic ordering and magnetocrystalline anisotropy in epitaxial Mn_2GaC MAX phase thin films, Phys. Rev. Mater. 7(2023)034409 https://DOI: 10.1103/PhysRevMaterials.7.034409.
9. E. B. Thorsteinsson, M. Dahlqvist , A. Elsukova, A. Petruhins , P. O. Å. Persson , J. Rosen, A. S. Ingason and F. Magnus, Room temperature ferromagnetism in the nanolaminated MAX phase $(Mn_{1-x}Cr_x)_2GaC$, APL Mater. 11(2023)121102 https://doi.org/10.1063/5.0176571.
10. M.Dahlqvist, A. S. Ingason, B. Alling, F. Magnus, A. Thore, A. Petruhins, A. Mockute, U. B. Arnalds, M. Sahlberg, B. Hjörvarsson, I. A. Abrikosov, and J. Rosen, Magnetically driven anisotropic structural changes in the atomic laminate Mn_2GaC,Phys. Rev. B 93(2016)014410 https://DOI: 10.1103/PhysRevB.93.014410.
11. M. Dahlqvist M. and J. Rosen, Impact of strain, pressure, and electron correlation on magnetism and crystal structure of Mn_2GaC from first-principles, Sci. Rep. 10(2020)11384 https://doi.org/10.1038/s41598-020-68377-5.
12. J. Dey, M. Wójcik, E. Jędryka, R. Kalvig, U. Wiedwald, R. Salikhov, M. Farle and J. Rosén, Non-collinear magnetic structure of the MAX phase Mn_2GaC epitaxial films inferred from zero-field NMR study (CE-5:L05) Ceramics International. 49(2023) 24235-24238, https://doi.org/10.1016/j.ceramint.2022.11.265.

13. J. Dey, E. Jędryka, R. Kalvig, U. Wiedwald, M. Farle, J. Rosén and M. Wójcik, Helical magnetic structure of epitaxial films of nanolaminated Mn_2GaC MAX phase, Phys. Rev.B 108(2023) 054413 https://DOI: 10.1103/PhysRevB.108.054413.
14. O. N. Draganyuk, N. G. Zamkova and and V. S. Zhandun, Effect of substitution of Mn and Ga atoms by Fe atom in the Mn_2GaC MAX phase, Journal of Magnetism and Magnetic Materials. 563(2022) 169860 https://doi.org/10.1016/j.jmmm.2022.169860.
15. D. V. Zyabkin, U. Vetter, F. M. A. Linderhof, H. P. Gunnlaugsson and P. Schaaf, eMIL: Advanced emission Mössbauer spectrometer for measurements in versatile conditions, Nucl. Instrum. Meth. A (968) (2020) 163973, https://doi.org/10.1016/j.nima.2020.163973.
16. P. Gütlich, E. Bill, and A. X. Trautwein (2010). Mössbauer spectroscopy and transition metal chemistry: fundamentals and applications. Springer Science & Business Media. https://doi.org/10.1007/978-3-540-88428-6.
17. I. Unzueta, , H.P. Gunnlaugsson, T.E. Mølholt, H. Masenda, A. Mokhles Gerami, P. Krastev, D,V. Zyabkin, K. Bharuth-Ram, D. Naidoo, S. Ólafsson, F. Plazaola, J. Schell, B. Qi, X. Zhao, J. Xiao, J. Zhao and R. Mantovan, Compositional Dependence of Epitaxial $L1_0$-Mn_xGa Magnetic Properties as Probed by ^{57}Mn/Fe and ^{119}In/Sn Emission Mössbauer Spectroscopy. Phys. Status Solidi B (2022) 2200121. https://doi.org/10.1002/pssb.202200121
18. H. P. Gunnlaugsson, G. Weyer, R. Mantovan, D. Naidoo, R. Sielemann, K. Bharuth-Ram, M. Fanciulli, K. Johnston, S. Olafsson and G. Langouche, Isothermal defect annealing in semiconductors investigated by time-delayed Mössbauer spectroscopy: application to ZnO, Hyperfine Interact. 188 (2009) 85–89, https://dx.doi.org/10.1007/s10751-008-9893-4.

Appendix

Details for the Technical Advisory Committee

3.1 General information

Describe the setup which will be used for the measurement. If necessary, copy the list for each setup used.

☒ Permanent ISOLDE setup: GLM beam line

☒ To be used without any modification

☐ To be modified: *Short description of required modifications.*

☒Travelling setup (*Contact the ISOLDE physics coordinator with details.*)

☒ Existing setup, used previously at ISOLDE: Emission Moessbauer Spectrometer from Ilmenau (eMIL).

☐ Existing setup, not yet used at ISOLDE: *Short description*

☐ New setup: *Short description*

3.2 Beam production

For any inquiries related to this matter, reach out to the target team and/or RILIS (please do not wait until the last minute!). For Letters of Intent focusing on element (or isotope) specific beam development, this section can be filled in more loosely.

- Requested beams:

Isotope	Production yield in focal point of the separator (/μC)	Minimum required rate at experiment (pps)	$t_{1/2}$
Isotope 1	^{57}Mn *1.5x10^{8} at/μC*	^{57}Mn *1x10^{8} at/μC*	1.5 min
Isotope 2	^{119}In *1.5x10^{8} at/μC*	^{119}In *1.5x10^{8} at/μC*	2.4 min
Isotope 3			

- Full reference of yield information (*yield database*)
- Target - ion source combination: UC_x with RILIS
- RILIS? (*Yes for element ^{57}Mn*)

  ☐ Special requirements: (*isomer selectivity, LIST, PI-LIST, laser scanning, laser shutter access, etc.*)

- Additional features?

  ☐Neutron converter: (*for isotopes 1, 2 but not for isotope 3.*)

  ☐ Other: (*quartz transfer line, gas leak for molecular beams, prototype target, etc.*)

- Expected contaminants: *Isotopes and yields*
- Acceptable level of contaminants: By using RILIS, no significant contaminants are expected.
- Can the experiment accept molecular beams? No.
- Are there any potential synergies (same element/isotope) with other proposals and LOIs that you are aware of? IS630, IS681, IS683, IS670.

3.3 HIE-ISOLDE

For any inquiries related to this matter, reach out to the ISOLDE machine supervisors (please do not wait until the last minute!).

- HIE ISOLDE Energy: *(MeV/u); (exact energy or acceptable energy range)*

  ☐ Precise energy determination required

  ☐ Requires stable beam from REX-EBIS for calibration/setup? *Isotope?*

- REX-EBIS timing

  ☐ Slow extraction

  ☐ Other timing requests

- Which beam diagnostics are available in the setup?
- What is the vacuum level achievable in your setup?

3.4 Shift breakdown

The beam request only includes the shifts requiring radioactive beam, but, for practical purposes, an overview of all the shifts is requested here. Don't forget to include:

- Isotopes/isomers for which the yield need to be determined
- Shifts requiring stable beam (indicate which isotopes, if important) for setup, calibration, etc. Also include if stable beam from the REX-EBIS is required.

An example can be found below, please adapt to your needs. Copy the table if the beam time request is split over several runs.

Summary of requested shifts:

With protons	Requested shifts

Yield measurement of isotope 1 Optimization of experimental setup using isotope 2 Data taking, isotope 1 Data taking, isotope 2 Data taking, isotope 3 Calibration using isotope 4	^{57}Mn 4.5 shifts ^{119}In 2.5 shifts
Without protons	Requested shifts
Stable beam from REX-EBIS (after run) Background measurement	0.5 shift for stable beam for every beam time with ^{135}Cs to GLM beam line: EqArr_2023_09_12_20_02_46_GLM-eMS-50kV_DP418_KI-520_135Cs.csv YGPS.BFC4900: 238 pA At least 90% of transmission expected at the Faraday cup of eMIL (traveling setup at the GLM beam line)

3.5 Health, Safety and Environmental aspects

3.5.1 Radiation Protection

- If radioactive sources are required:
  - Purpose? Online experiment with ^{57}Mn.
  - Isotopic composition? ^{57}Mn.
  - Activity? 300 MBq online with no manipulation. Manipulation with only 30 kBq according to the existing and approved procedure.
  - Sealed/unsealed? Unsealed.
- For collections:
  - Number of samples? 2-4.

- Activity/atoms implanted per sample? 300 MBq online with no manipulation. Manipulation with only 30 kBq according to the existing and approved procedure.
- Post-collection activities? (*shipping.*)

3.5.2 Only for traveling setups

- Design and manufacturing

☐Consists of standard equipment supplied by a manufacturer

☒CERN/collaboration responsible for the design and/or manufacturing. ISIEC file of eMIL can be found at EDMS: 1317710.

- Describe the hazards generated by the experiment:

Domain	Hazards/Hazardous Activities		Description
Mechanical Safety	Pressure	☐	[pressure] [bar], [volume][l]
	Vacuum	☒	10^{-5} mbar
	Machine tools	☒	The alignment of eMIL with the GLM beam line requires the adjustment of the equipment height.
	Mechanical energy (moving parts)	☒	Stepping motor of four-positions lid.
	Hot/Cold surfaces	☒	Cold surface for liquid N_2 experiments. Hot lid does not cause hot surface.
Cryogenic Safety	Cryogenic fluid	☒	Liquid N_2 (approximately 4 liters per load)
Electrical Safety	Electrical equipment and installations	☒	Several devices, please consultthe safety file

			EDMS 1317710 for details.
	High Voltage equipment	☒	Detector 1000 V DC with current being less than 1 nA.
Chemical Safety $(Mn_xCr_{1-x})_2GaC$ (x=0, 0.12...0.29) thin films (140-220 nm thick) on MgO(111) substrate	CMR (carcinogens, mutagens and toxic to reproduction)	☐	[fluid], [quantity]
	Toxic/Irritant	☐	[fluid], [quantity]
	Corrosive	☐	[fluid], [quantity]
	Oxidizing	☐	[fluid], [quantity]
	Flammable/Potentially explosive atmospheres	☐	[fluid], [quantity]
	Dangerous for the environment	☐	[fluid], [quantity]
Non-ionizing radiation Safety	Laser	☐	[laser], [class]
	UV light	☐	
	Magnetic field	☒	0.6 T
Workplace	Excessive noise	☒	General ISOLDE hall background noise.
	Working outside normal working hours	☒	According to the ISOLDE schedule.
	Working at height (climbing platforms, etc.)	☐	
	Outdoor activities	☐	
Fire Safety	Ignition sources	☐	
	Combustible Materials	☐	
	Hot Work (e.g. welding, grinding)	☒	Measurements of samples using the hot lid (cold surface).
Other hazards	^{57}Mn (high energy beta emitter)		